Hindawi Publishing Corporation
International Journal of Antennas and Propagation
Volume 2008, Article ID 854012, 6 pages
doi:10.1155/2008/854012

Research Article

Directive Antenna for Ultrawideband Medical Imaging Systems

Amin M. Abbosh

School of Information Technology and Electrical Engineering, The University of Queensland, St. Lucia, Qld 4072, Australia

Correspondence should be addressed to Amin M. Abbosh, abbosh@itee.uq.edu.au

Received 19 July 2007; Revised 10 October 2007; Accepted 22 January 2008

Recommended by Elise Fear

A compact and directive ultrawideband antenna is presented in this paper. The antenna is in the form of an antipodal tapered slot with resistive layers to improve its directivity and to reduce its backward radiation. The antenna operates over the frequency band from 3.1 GHz to more than 10.6 GHz. It features a directive radiation with a peak gain which is between 4 dBi and 11 dBi in the specified band. The time domain performance of the antenna shows negligible distortion. This makes it suitable for the imaging systems which require a very short pulse for transmission/reception. The effect of the multilayer human body on the performance of the antenna is also studied. The breast model is used for this purpose. It is shown that the antenna has more than 90% fidelity factor when it works in free space, whereas the fidelity factor decreases as the signal propagates inside the human body. However, even inside the human body, the fidelity factor is still larger than 70% revealing the possibility of using the proposed antenna in biomedical imaging systems.

1. INTRODUCTION

Ultrawideband (UWB) (3.1–10.6 GHz) microwave imaging is a promising method for biomedical applications such as cancer detection because of their good penetration and resolution characteristics. The underlying principle of UWB cancer detection is a significant contrast in dielectric properties, which is estimated to be greater than 2 : 1 between normal and cancerous tissue. UWB imaging systems have shown encouraging results in the detection of tumors for early breast-cancer detection [1].

In the UWB imaging systems, a very narrow pulse is transmitted from a UWB antenna to penetrate the body. As the pulse propagates through the various tissues, reflections and scattering occur at the interfaces. A particular interest is in the scattered signal from a small size-tissue representing a tumor. The reflected and scattered signals can be received using an UWB antenna, or array of antennas, and used to map different layers of the body. For an accurate imaging system with high resolution and dynamic range, the transmitting/receiving UWB antenna should be planar, compact in size, and directive with high-radiation efficiency and distortionless pulse transmission/reception.

The majority of the compact UWB antennas presented in the literature exhibit omnidirectional radiation patterns with relatively low gain and an impulse response with observable distortion [2]. These types of UWB antennas are suitable for the short-range indoor and outdoor communication. However, for radar systems, such as an UWB microwave imaging system for detection of tumor in woman's breast, a moderate gain directional antenna is advantageous. In addition to an UWB impedance bandwidth, as defined by the minimum return loss of the 10 dB, the UWB antenna is required to support a very short pulse transmission with negligible distortion. This is necessary to achieve precision imaging without ghost targets. The unipolar and antipodal Vivaldi antennas presented in the literature [3–5] satisfy the requirements for imaging systems in terms of bandwidth, gain, and impulse response. However, the achieved performance is at the expense of a significant size, which has a length of several wavelengths. Therefore, the challenge is to reduce their physical dimensions such that it can be incorporated in a compact microwave imaging detection system, while maintaining its broadband, high-gain, and distortionless performance.

Several UWB antenna designs with compact size and low distortion have been proposed for the use in the medical

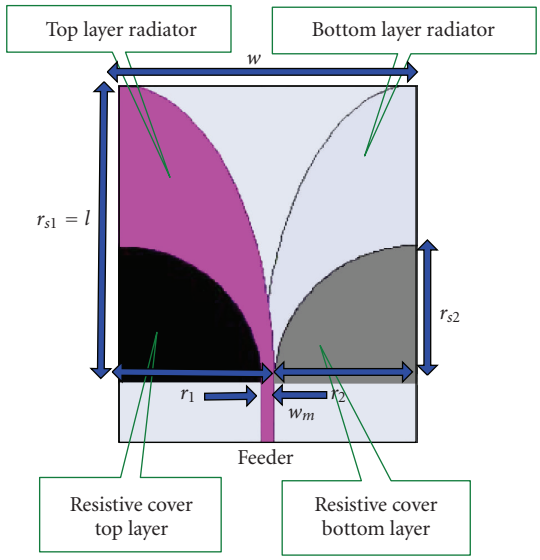

Figure 1: Configuration of the proposed antenna.

imaging systems [6–8]. Each has its own merits and drawbacks. Some of the proposed antennas have a nonplanar structure, whereas others have low-gain and/or low-radiation efficiency. The low-radiation efficiency is a major impairment that limits the dynamic range of the imaging system, whose major objective is to detect a weak backscatter from a tumor.

In the presented work, a compact (5 cm × 5 cm) elliptical tapered slot UWB antenna is described. A clear design guideline is given in order to show how to calculate values of the different design parameters of the antenna. Resistive layers were incorporated with the radiating elements of the antenna to improve its directivity and reduce any backward radiation which may affect the accuracy of the imaging system. The measured and simulated results of the proposed antenna show an ultrawideband behavior with a moderate gain and distortionless pulse transmission/reception.

2. DESIGN

The antenna presented in this paper is to be used in a microwave imaging for breast-cancer detection. The imaging system includes a circular array of the proposed ultrawideband antenna. In this system, one of the antennas is used to transmit a microwave signal while the rest of the antennas in the array receive the scattered signal. The measured data is collected and then the measurement procedure is repeated with the second transmitting the signal while the remaining are used for receiving the scattered signal. This process is repeated until all antennas in the array perform the transmitting role. The antenna array can be moved up and down automatically via a computer-controlled high-precision linear actuator. This facilitates the collection of multiple planar data for 3D object imaging.

The proposed ultrawideband antenna for inclusions in the UWB microwave imaging system is shown in Figure 1. It resembles an antipodal tapered slot antenna fed by a parallel strip line.

The radiating element is in the form of an antipodal planar tapered slot with an elliptical curvature. Rogers RO4003 with 3.38 dielectric constant and 0.508 mm thickness was used as a substrate. A resistive layer of 50 Ω/□ was sprayed at the designated areas at the lower end of the radiating structure in the top and bottom layers to improve the front-to-back ratio, and thus the detection capabilities of the UWB imaging system.

The design objective is to obtain a directive antenna with a compact size, while maintaining the bandwidth requirement of 3.1 to 10.6 GHz. The following design procedure is proposed and utilized in developing the proposed antipodal antenna.

Step 1. Given the lowest frequency of operation (f_l), thickness of the substrate (h) and its dielectric constant (ε_r), the width (w) and length (l) of the antenna structure, excluding the feeder, can be calculated using the following equation [9]:

$$w = l = \frac{c}{f_l}\sqrt{\frac{2}{\varepsilon_r + 1}}, \tag{1}$$

where c is the speed of light in free space.

It is worthwhile to mention that (1) indicates that the antenna's length and width is chosen to be equal to the effective wavelength calculated at the lowest frequency of operation.

Step 2. The radiating structure of the antenna is formed from the intersection of quarters of two ellipses. The major radii (r_1 and r_2) and the secondary radii (r_{s1} and r_{s2}) of the two ellipses are chosen according to the following equation:

$$\begin{aligned} r_1 &= \frac{w}{2} + \frac{w_m}{2}, \\ r_2 &= \frac{w}{2} - \frac{w_m}{2}, \\ r_{s1} &= l, \\ r_{s2} &= 0.5 r_2. \end{aligned} \tag{2}$$

According to (2), dimensions of the radiating element are chosen such that the far-end distance between the top and bottom radiators is equal to the effective wavelength at the lowest frequency of operation. Length of each of the radiators at the left and the right end of the antenna's structure shown in Figure 1 is equal to half of the effective wavelength calculated at the lowest frequency of operation.

Step 3. The width of the microstrip transmission feeder (w_m) to give the characteristic impedance, Z_o equal to 50 Ω, can be calculated using the following equations [10]:

$$w_m = \frac{120\pi}{\sqrt{\varepsilon_r}}\frac{h}{Z_o}. \tag{3}$$

Step 4. A metallization layer, with a 50 Ω/□ surface resistivity, is added to the top and bottom radiating parts. Shape of the resistive layers is chosen to be a quarter of an ellipse with major and secondary diameters equal to r_2 and r_{s2}, respectively.

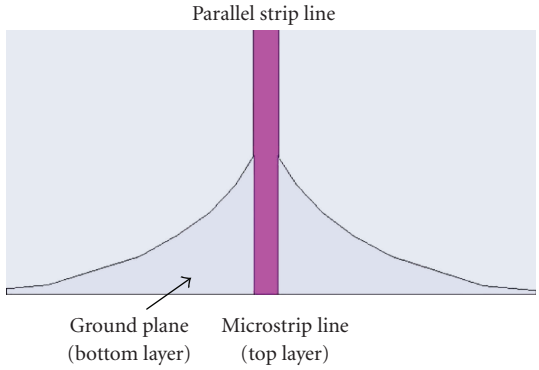

Figure 2: Configuration of the parallel strip line to microstrip transition.

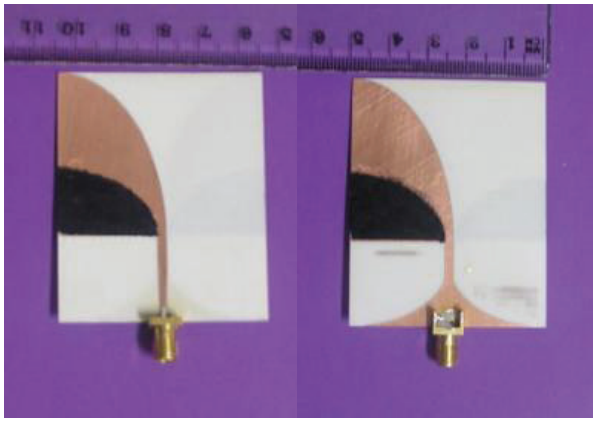

(a) (b)

Figure 3: Photo of the developed antenna: (a) top view, and (b) bottom view.

Step 5. A transition is added to the structure of the antenna. This is required because the antenna's radiating element shown in Figure 1 is connected to a parallel strip line, which is a balanced transmission line, whereas the antenna is to be connected to the other devices of the imaging system using a suitable coaxial cable, which is an unbalanced transmission line. The transition from the parallel strip line to the microstrip line is shown in Figure 2, which is adopted from the transitions presented in [11]. The strip line, which is located at the top layer, is connected using a tapered transmission line to the microstrip line, while width of the strip line at the bottom layer is gradually increased to form the ground plane required for the microstrip feeder.

3. RESULTS

The ultrawideband antenna designed according to the above mentioned procedure was manufactured using Rogers RO4003C ($\varepsilon_r = 3.38$, $h = 0.506$ mm) as a substrate. Values of the design parameters w, l, r_1, r_2, r_{s1}, r_{s2}, and w_m (shown in Figure 1) are 50 mm, 50 mm, 26 mm, 24 mm, 50 mm, 12 mm, and 2 mm, respectively. A photo for the developed antenna is shown in Figure 3.

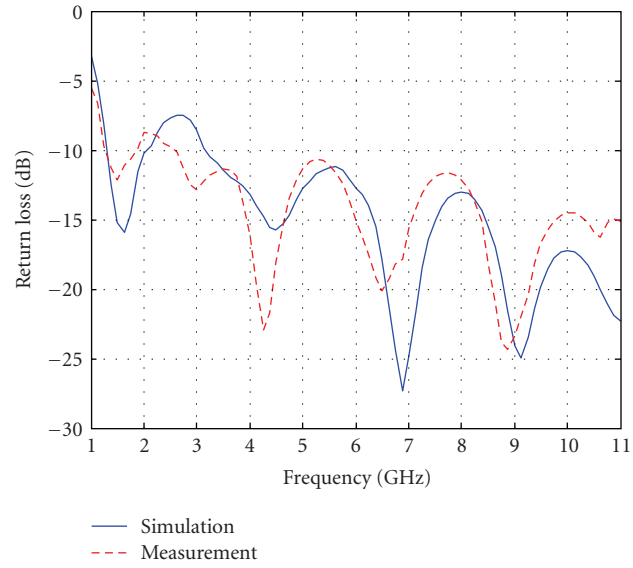

Figure 4: The measured and simulated return loss.

Concerning the resistive layers, a parametric analysis using the software Ansoft HFSSv10 indicated that the best performance concerning the bandwidth and the front-to-back ratio can be achieved when the resistivity of the added resistive layer is in the range from 50 to 100 Ω/□ . The lower value was used because of the availability of the 50 Ω/□ chemical mixture to the author.

The validity of the proposed design methodology is verified using the commercial software package, Ansoft HFSSv10, and experimental tests by using a vector network analyzer.

Figure 4 shows the simulated and measured return loss of the manufactured antenna. As can be seen from Figure 3, the 10 dB return loss bandwidth extends from 3.1 GHz to more than 11 GHz covering the required UWB band of 3.1 GHz–10.6 GHz. The simulated result closely resembles the measured result validating the design procedure of the antenna.

The far-field radiation patterns of the antenna were calculated using the software HFSS. They are shown in Figure 5 for the frequencies 4 GHz, 6 GHz, 9 GHz, and 11 GHz. The antenna shows directive properties with an average front-to-back ratio which is greater than 13 dB across the whole band, making it a good candidate for microwave imaging applications. It is worthwhile to mention that without the use of the resistive layers, the front-to-back ratio is around 10 dB.

The measured gain of the antenna is shown in Figure 6, which reveals a moderate gain antenna. The gain is equal to 4.3 dBi at 3 GHz and it increases with frequency till it becomes 10.8 dBi at 10.6 GHz. It is to be noted that the gain measurements were done in comparison with a reference-gain antenna which is the corrugated horn antenna in this case.

As the use of the resistive layer can be responsible for the reduction in the radiation efficiency, suitable calculations with the help of the software HFSS were performed with respect to this parameter. From Figure 6, it is apparent that despite the use of the resistive layers to minimize the backward

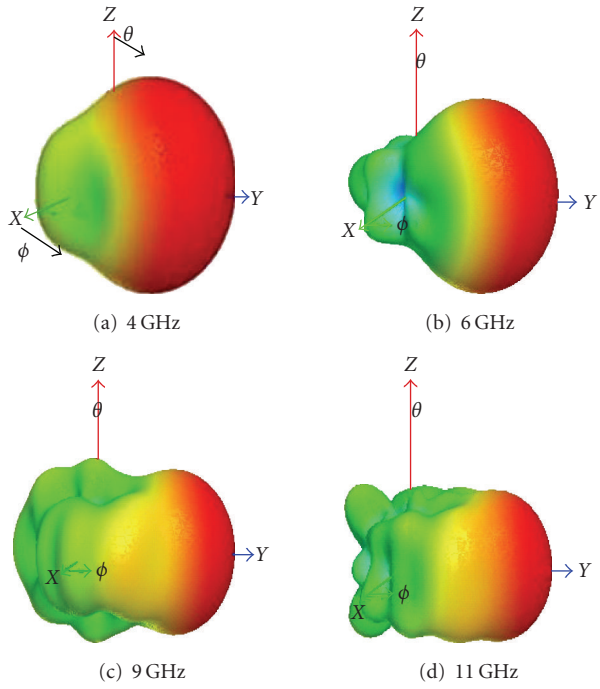

Figure 5: The simulated three-dimensional radiation pattern.

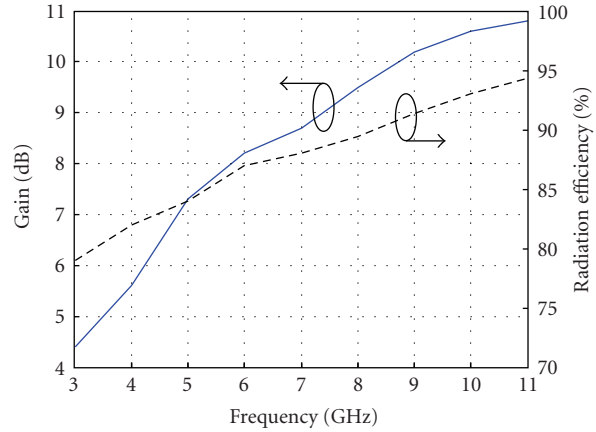

Figure 6: The measured gain and calculated radiation efficiency of the antenna.

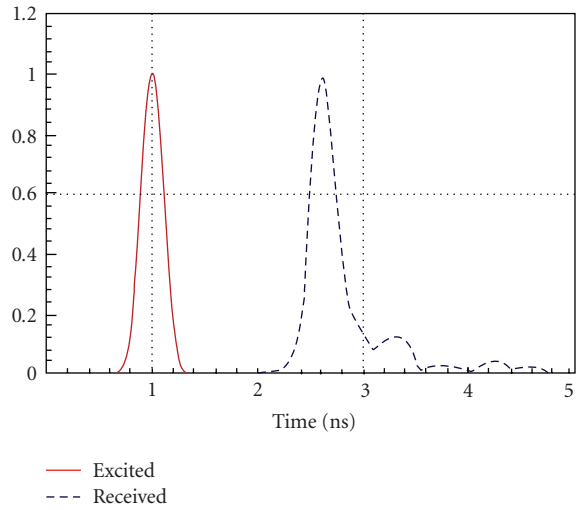

Figure 7: The measured impulse response of the antenna.

radiation (and hence enhance the front-to-back ratio), the proposed antenna has a good efficiency, which is more than 80% across the whole band. This performance is superior in comparison with the antennas reported for use in a microwave imaging system, where 47% efficiency was noted [8].

The time-domain performance of the proposed antenna was also measured. A narrow pulse was synthesized in the network analyzer using the discrete Fourier transform module of the device. The pulse was synthesized after assuming that its frequency spectrum is a rectangular function that extends from 3.1 to 10.6 GHz. Shape of the resulted synthesized pulse is shown in Figure 7. Two copolarized antennas were separated by a distance of 50 cm and the results of the measurement are shown in Figure 7. Note that the excited pulse and the received pulse are normalized with respect to their peak values. The figure reveals that the pulse duration of the antenna is 0.6 nanoseconds. The pulse distortion occurs at the 0.15 level with respect to the peak level of 1, and thus it is almost negligible. The observed results indicate that the developed antenna supports distortionless narrow pulse which makes it an excellent radiator for the purpose of a microwave imaging with high resolution.

As the antenna is to be put on or near the human body, specifically the breast for the case of breast-cancer detection, a study of the effect of the distance from the skin to the antenna on its return loss is investigated. The electromagnetic model used to simulate the breast contains two layers: the first layer is the skin layer with thickness = 2 mm, dielectric constant = 36, and conductivity = 4 S/m. The second layer is the breast tissue, which extends to a width of 10 cm, with a dielectric constant = 9 and conductivity = 0.4 S/m [12]. Results of simulation using the software HFSS are shown in Figure 8 for two different distances between the antenna and the human body. Figure 8 indicates clearly that the antenna maintains its ultrawideband performance in spite of being very close to the human body.

The imaging system in which the antenna is to be used contains an array of antennas. Hence, it is important to investigate the value of the mutual coupling between these antennas. The mutual coupling between two identical antennas at different frequencies was calculated using the software HFSS. In the calculations, two antennas were assumed to be parallel to each other and the distance between them was changed. The mutual coupling was calculated at each distance and the results are shown in Figure 9. These results show that the coupling decreases as the distance between the two antennas increases. For a certain distance between the two antennas, the mutual coupling is less for a higher frequency. This is because increasing the frequency means a lower wavelength. Therefore, the distance between the coupled antennas relative to the wavelength is larger. The results depicted in Figure 9 reveal that the mutual coupling between the neighboring antennas at any frequency within the ultrawideband range is less than −20 dB when the distance between the antennas is more than half a wavelength.

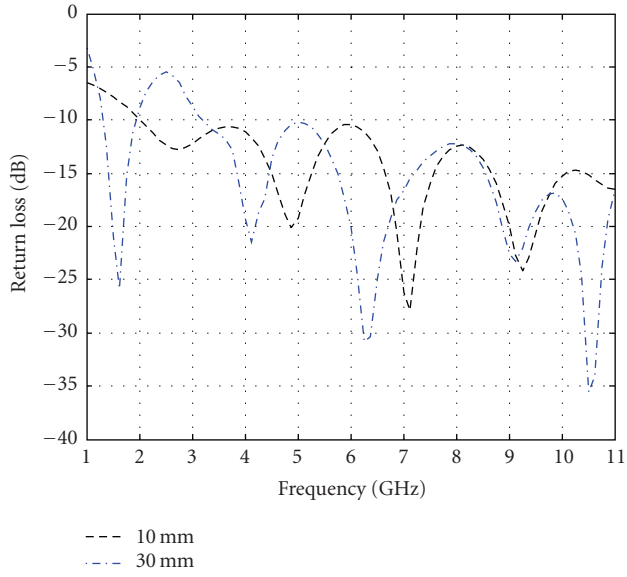

Figure 8: The simulated return loss of the antenna for different distances from the human body.

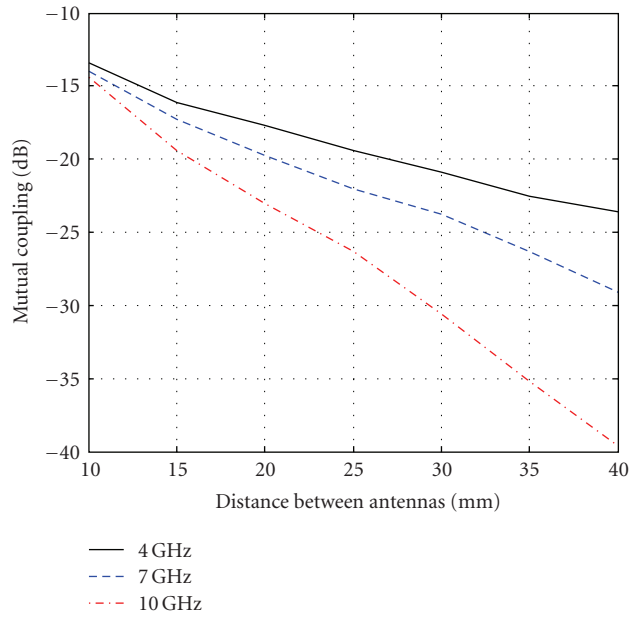

Figure 9: Variation of the simulated mutual coupling with the distance between the antennas at different frequencies.

It is also important to study the distortion when the radiated pulse propagates through the human body, that is, the skin and the breast tissue in the case of the breast-cancer-detection system. The antenna fidelity is used as an indication of that distortion. The fidelity factor is the maximum magnitude of the cross correlation between the observed pulse at a certain distance and the excitation pulse [13]. The finite difference time-domain method was used for this purpose [14]. In order to reduce the computation domain, Berenger's perfectly matched layer (PML) is applied as an absorbing boundary condition [15]. To include the frequency dependence of the dielectric constant ε_i and the conductivity σ_i of the breast tissue over the UWB, the first-order Debye dispersion model was applied [12]:

$$\varepsilon_i - \frac{j\sigma_i}{2\pi f \varepsilon_o} = \varepsilon_\infty + \frac{\varepsilon_\Delta - \varepsilon_\infty}{1 + j2\pi f \tau} - \frac{j\sigma_\Delta}{2\pi f \varepsilon_o}, \quad (4)$$

where τ is the relaxation time, and ε_Δ, ε_∞, and σ_Δ are the Debye model parameters which were selected according to the published data for the breast tissues [12]: normal tissue: $\varepsilon_\Delta = 10$, $\varepsilon_\infty = 7$, $\tau = 7\,\text{ps}$, $\sigma_\Delta = 0.15\,\text{S/m}$, tumor: $\varepsilon_\Delta = 54$, $\varepsilon_\infty = 4$, $\tau = 7\,\text{ps}$, $\sigma_\Delta = 0.4\,\text{S/m}$. For the skin: $\varepsilon = 36$, and $\sigma = 4\,\text{S/m}$.

The result is shown in Figure 10 where the effect of all the scattered/reflected signals is included. It indicates that as the signal propagates through the human body, the fidelity factor decreases. This indicates an increasing pulse distortion inside the human body. For the antenna presented in this paper, the fidelity factor is within reasonable values (more than 70%) even inside the human body.

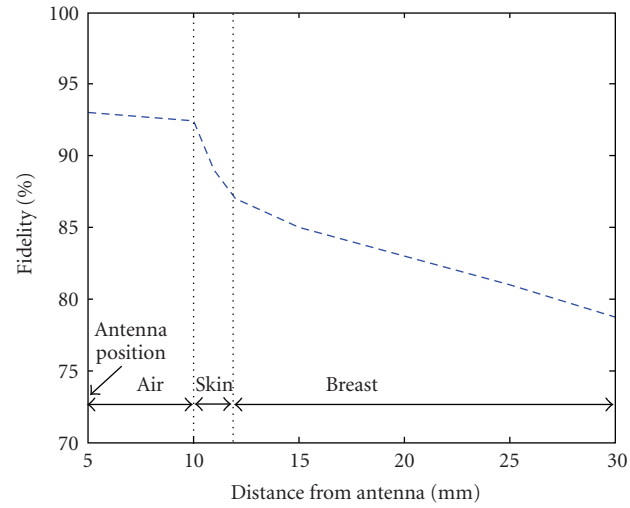

Figure 10: The simulated fidelity factor with the distance from the antenna in the presence of a human body.

4. CONCLUSION

The design of a directive ultrawideband antenna for use in a microwave imaging system has been presented. To minimize the backward radiation, the antenna uses resistive layers behind its conductive radiation layers. The simulated and measured characteristics of the antenna have shown that it covers the band from 3.1 GHz to more than 11 GHz. It has a radiation efficiency of more than 80%, which is higher than the recently reported other UWB planar antennas employing resistive layers for microwave imaging applications. The characteristics of the antenna when operating near a human body have been investigated. The simulated results have shown that the antenna maintains its ultrawideband performance concerning the return loss even with the presence of the human body in proximity with the antenna.

The time-domain performance of the antenna has also been studied. It has been shown that the proposed antenna

has the ability to send and receive very short pulses in a distortionless manner. It has been shown that although the fidelity factor decreases as the signal propagates through the human body, the value of that factor is still within acceptable limits.

The mutual coupling between two identical antennas has been simulated as the antenna elements are used within an array in the microwave imaging systems. It has been shown that the mutual coupling is less than -20 dB when the distance between the neighboring antennas is more than half a wavelength.

REFERENCES

[1] E. C Fear, P. M Meaney, and M. A. Stuchly, "Microwaves for breast cancer detection?" *IEEE Potentials*, vol. 22, no. 1, pp. 12–18, 2003.

[2] J. Liang, C. C. Chiau, X. Chen, and C. G. Parini, "Printed circular disc monopole antenna for ultra-wideband applications," *Electronics Letters*, vol. 40, no. 20, pp. 1246–1247, 2004.

[3] J. D. S. Langley, P. S. Hall, and P. Newham, "Balanced antipodal Vivaldi antenna for wide bandwidth phased arrays," *IEE Proceedings: Microwaves, Antennas and Propagation*, vol. 143, no. 2, pp. 97–102, 1996.

[4] E. Guillanton, J. Y. Dauvignac, Ch. Pichot, and J. Cashman, "A new design tapered slot antenna for ultra-wideband applications," *Microwave and Optical Technology Letters*, vol. 19, no. 4, pp. 286–289, 1998.

[5] M. Chiappe and G. L. Gragnani, "Vivaldi antennas for microwave imaging: theoretical analysis and design considerations," *IEEE Transactions on Instrumentation and Measurement*, vol. 55, no. 6, pp. 1885–1891, 2006.

[6] X. Yun, E. C. Fear, and R. Johnston, "Broadband cross-polarized bowtie antenna for breast cancer detection," in *Proceedimgs of IEEE Antennas and Propagation Society International Symposium*, vol. 3, pp. 1091–1094, Columbus, Ohio, USA, June 2003.

[7] C. J. Shannon, E. C. Fear, and M. Okoniewski, "Dielectric-filled slotline bowtie antenna for breast cancer detection," *Electronics Letters*, vol. 41, no. 7, pp. 388–390, 2005.

[8] H. Kanj and M. Popovic, "Miniaturized microstrip-fed "Dark Eyes" antenna for near-field microwave sensing," *IEEE Antennas and Wireless Propagation Letters*, vol. 4, pp. 397–401, 2005.

[9] A. M. Abbosh, H. K. Kan, and M. E. Bialkowski, "Compact ultra-wideband planar tapered slot antenna for use in a microwave imaging system," *Microwave and Optical Technology Letters*, vol. 48, no. 11, pp. 2212–2216, 2006.

[10] D. M. Pozar, *Microwave Engineering*, John Wiley & Sons, New York, NY, USA, 3rd edition, 2005.

[11] S.-G. Kim and K. Chang, "Ultrawide-band transitions and new microwave components using double-sided parallel-strip lines," *IEEE Transactions on Microwave Theory and Techniques*, vol. 52, no. 9, part 1, pp. 2148–2152, 2004.

[12] S. K. Davis, H. Tandradinata, S. C. Hagness, and B. D. Van Veen, "Ultrawideband microwave breast cancer detection: a detection-theoretic approach using the generalized likelihood ratio test ," *IEEE Transactions on Biomedical Engineering*, vol. 52, no. 7, pp. 1237–1250, 2005.

[13] D. Lamensdorf and L. Susman, "Baseband-pulse-antenna techniques," *IEEE Antennas and Propagation Magazine*, vol. 36, no. 1, pp. 20–30, 1994.

[14] D. M. Sullivan, *Electromagnetic Simulation Using the FDTD Method*, John Wiley & Sons, New York, NY, USA, 2000.

[15] J.-P. Berenger, "A perfectly matched layer for the absorption of electromagnetic waves," *Journal of Computational Physics*, vol. 114, no. 2, pp. 185–200, 1994.